THE JOURNAL OF IMMUNOLOGY

Selective Sequestration of STAT1 in the Cytoplasm via Phosphorylated SHP-2 Ameliorates Murine Experimental Colitis

Xingxin Wu, Wenjie Guo, Limei Wu, Yanhong Gu, Liyun Gu, Suhai Xu, Xuefeng Wu, Yan Shen, Yuehai Ke, Renxiang Tan, Yang Sun and Qiang Xu

J Immunol published online 31 August 2012
http://www.jimmunol.org/content/early/2012/08/31/jimmunol.1201006

The Journal of Immunology is published twice each month by The American Association of Immunologists, Inc., 9650 Rockville Pike, Bethesda, MD 20814-3994.

Print ISSN: 0022-1767 Online ISSN: 1550-6606.

Published August 31, 2012, doi:10.4049/jimmunol.1201006

Selective Sequestration of STAT1 in the Cytoplasm via Phosphorylated SHP-2 Ameliorates Murine Experimental Colitis

Xingxin Wu,*,[1] Wenjie Guo,*,[1] Limei Wu,* Yanhong Gu,[†] Liyun Gu,* Suhai Xu,* Xuefeng Wu,* Yan Shen,* Yuehai Ke,[‡] Renxiang Tan,* Yang Sun,* and Qiang Xu*

The side effects of current immunosuppressive drugs have impeded the development of therapies for immune diseases. Selective regulation of STAT signaling is an attractive strategy for treating immune disorders. In this study, we used a small-molecule compound to explore possible means of targeting STAT1 for the treatment of Th1-mediated inflammation. Selective regulation of STAT1 signaling in T cells from C57BL/6 mice was accomplished using fusaruside, a small-molecule compound that triggers the tyrosine phosphorylation of Src homology 2-containing protein tyrosine phosphatase 2 (SHP-2). The interaction of tyrosine phosphorylated SHP-2 (pY-SHP-2) with cytosolic STAT1 prevented the recruitment of STAT1 to IFN-γR and specifically inhibited STAT1 signaling, resulting in a reduction in Th1 cytokine production and an improvement in 2, 4, 6-trinitrobenzene sulfonic acid-induced colitis in mice. Blocking the pY-SHP-2–STAT1 interaction, with SHP-2 inhibitor NSC-87877 or using T cells from conditional SHP-2 knockout mice, reversed the effects of fusaruside, resulting in STAT1 activation and worsened colitis. The fusaruside-induced ability of pY-SHP-2 to selectively sequestrate STAT1 from recruitment to the receptor is independent of its function as a phosphatase, demonstrating a novel role for SHP-2 in regulating both STAT1 signaling and Th1-type immune responses. These findings could lead to increased options for the treatment of Crohn's disease and other Th1-mediated inflammatory diseases. ***The Journal of Immunology*****, 2012, 189: 000–000.**

Signaling through IFN-γ, STAT1, and T-box expressed in T cells (T-bet) is usually involved in Th1-mediated inflammation. IFN-γ signaling plays a pathogenic role in Crohn's disease (1). The absence of STAT1 in mice reduces the intensity of experimental colitis (2), and T-bet$^{-/-}$ T cells fail to induce colitis in adoptive-transfer experiments (3). For these reasons, many studies have focused on ways to regulate STAT1 signaling to control immune diseases (4, 5). A variety of chemicals was reported to inhibit STAT1 signaling (6–11); however, inhibition by these agents is usually nonspecific. For example, fludarabine inhibits both STAT1 and STAT3 (7, 12); rapamycin inhibits STAT1, STAT3, and STAT4 (9, 13); cyclosporine A inhibits STAT1, STAT3, STAT4, STAT5, and STAT6 (8, 10, 14–16); glucocorticoids strongly inhibit STAT1, STAT4, and STAT5 (17, 18); and β-glucosylceramide reduces STAT1 and STAT4 but induces STAT6 expression (19). The signaling pathways mediated by some STATs play a protective role in immune diseases, such as STAT1/STAT2 signaling in antiviral defense (20), STAT3 signaling in anti-inflammatory responses (21, 22), STAT5 signaling in regulating a wide range of gene expression (23, 24), and STAT6 signaling in controlling dextran sulfate sodium-induced colitis (25). The broad targeting of multiple STATs by current immunosuppressants may cause side effects, thereby limiting their clinical applications (5). For example, dexamethasone can aggravate acute dextran sulfate sodium-induced colitis (26), which might be linked to the inhibition of STAT6 activation. Therefore, the specific inhibition of a critical STAT protein that is involved in pathogenesis is highly desirable. However, no agent or molecular pathway capable of selective STAT targeting has been reported.

Src homology 2-containing protein tyrosine phosphatase 2 (SHP-2), a ubiquitous tyrosine phosphatase, attenuates inflammatory responses (27–29) and has been identified as a proto-oncogene in several types of leukemia (30, 31). However, recent work identified SHP-2 as a tumor suppressor in hepatocellular carcinogenesis (32), suggesting that SHP-2 has dual functions in various types of diseases. Some functions of SHP-2 are related to its phosphatase activity, such as the dephosphorylation of STAT1 and STAT5, which inhibits the inflammatory response (33, 34). Many functions of SHP-2 cannot be explained by its phosphatase activity alone (35, 36); however, its catalytic-independent activity has not been well established.

In this study, we report a previously unexplored mechanism that selectively inhibits the trafficking of STAT1. Tyrosine phosphorylation of SHP-2, triggered by the small-molecule compound, fusaruside (37), causes tyrosine phosphorylated (pY) SHP-2 (pY-SHP-2) to selectively bind to nonphosphorylated STAT1 in the

*State Key Laboratory of Pharmaceutical Biotechnology, School of Life Sciences, Nanjing University, Nanjing 210093, China; [†]Department of Clinical Oncology, First Affiliated Hospital of Nanjing Medical University, Nanjing 210029, China; and [‡]Laboratory of Cell Signaling and Modeling Genetics, Department of Basic Medical Sciences, Institute of Molecular Pathology, School of Medicine, Zhejiang University, Hangzhou 310058, China

[1]X.W. and W.G. contributed equally to this work.

Received for publication April 4, 2012. Accepted for publication August 5, 2012.

This work was supported by grants from the Science Fund for Creative Research Groups (81121062), the National Natural Science Foundation of China (90913023, 81173070, and 91129728), National Science and Technology Major Project (2012ZX09304-001), and the Provincial Natural Science Foundation of Jiangsu (BK2008022).

Address correspondence and reprint requests to Dr. Qiang Xu and Dr. Yang Sun, School of Life Sciences, Nanjing University, 22 Han Kou Road, Nanjing 210093, China. E-mail addresses: molpharm@163.com (Q.X.) and yangsun@nju.edu.cn (Y.S.)

The online version of this article contains supplemental material.

Abbreviations used in this article: GATA3, GATA-binding protein 3; MLN, mesenteric lymph node; pY, tyrosine phosphorylated; SHP-2, Src homology 2-containing protein tyrosine phosphatase 2; T-bet, T-box expressed in T cells; TNBS, 2, 4, 6-trinitrobenzene sulfonic acid; Treg, regulatory T cell.

cytosol, but not to pY-STAT1 in the nucleus, preventing STAT1 recruitment for phosphorylation and inhibiting STAT1 signaling. Our findings reveal a novel role for activated SHP-2 in the regulation of STAT1 signaling via the selective sequestration of STAT1 in the cytosol. This new function of SHP-2 does not involve its phosphatase activity and contributes to an improvement in Th1-type intestinal inflammation.

Materials and Methods

Reagents

Fusaruside was isolated with 99% purity from the endophytic fungus *Fusarium* sp. IFB-121 in *Quercus variabilis* without bacterial contaminants. The chemical structure is shown in Fig. 1A (37). Mouse CD4 (L3T4) MicroBeads were purchased from Miltenyi Biotec (Bergisch Gladbach, Germany). 2, 4, 6-trinitrobenzene sulfonic acid (TNBS), Con A, and dexamethasone were purchased from Sigma-Aldrich (St. Louis, MO). Recombinant cytokines, including IL-12, IL-4, IL-6, TGF-β, IL-2, and IFN-γ, were purchased from R&D Systems (Minneapolis, MN). NSC-87877 was purchased from Calbiochem (La Jolla, CA). Anti-STAT1 (9H2), phospho-STAT (including phospho-STAT1, 3, 4, 5, and 6) Ab sampler kit, and anti–pY580-SHP-2 were purchased from Cell Signaling Technology (Beverly, MA). Anti-CD3, anti-CD28, anti–IFN-γ mAb, anti–CD4-PE, anti–CD45RB-FITC, anti–IL-12 mAb, anti–IL-4 mAb, anti-STAT1, and anti–SHP-2 were purchased from BD Pharmingen (San Diego, CA). Anti–IFN-γRα, anti-actin, and anti-GAPDH were purchased from Santa Cruz Biotechnology (Santa Cruz, CA).

Plasmids

pCMV-SHP-2-HA (1–593, plasmid 8381) and STAT1α Flag pRc/CMV (1–750, plasmid 8691) plasmids were purchased from Addgene (Cambridge, MA). To generate SHP-2-HA (1–220) and SHP-2-HA (221–593) plasmids, pCMV-SHP-2-HA (1–593) was amplified by PCR with primers: SHP-2-HA (1–220), 5′-CCCAAGCTTATGACATCGCGGAGATGGT-3′ and 5′-CTAGTCTAGACTAAGCGTAATCTGGAACATCGTATGGGTAACGAG-TCGTGTTAAGGG-3′ and SHP-2-HA (221–593), 5′-ACTATAGGGAGA-CCCAAGCTTATGATAAATGCTGCTGAAATAGAAAGCA-3′ and 5′-TA-TAGAATAGGGCCCTCTAGATCATCTGAAACTTTTCTGCTGTTG-3′. The PCR products were digested by HindIII and XbaI (TaKaRa, Dalian, China) and cloned into HindIII/XbaI-digested pCMV-SHP-2-HA (1–593) vector. To generate STAT1-Flag (1–488) and STAT1-Flag (489–750) plasmids, STAT1α-Flag pRc/CMV (1–750) was amplified by PCR with primers: STAT1-Flag (1–488), 5′-ATAAGAATGCGGCCGCATGTCTC-AGTGGTACGAACTT-3′ and 5′-TGTGGGCCCTACTTGTCATCGTCG-TCCTTGTAGTCCAGGAAGAAGGACAGAT-3′; STAT1-Flag (489-750), 5′-ACTATAGGGAGACCCAAGCTTATGACTCCACCATGTGCACGATG-3′ and 5′-TATAGAATAGGGCCCTCTAGACTATACTGTGTTCATCATAC-TGTCGAATTC-3′. The PCR products were digested by NotI and ApaI (TaKaRa, Dalian, China) and cloned into NotI/ApaI-digested STAT1α Flag pRc/CMV (1–750) vector.

Animals

Eight- to ten-week-old male C57BL/6 mice were purchased from the Institute of Laboratory Animal Science, Chinese Academy of Medical Sciences. Animal care was in compliance with the guide (Ministry of Science and Technology of China, 2006) and the related ethical regulations of Nanjing University.

Primary CD4$^+$ T cell purification

CD4$^+$ T cells were purified from spleen or lymph nodes of C57BL/6 mice using CD4 (L3T4) MicroBeads (Miltenyi Biotec), according to the manufacturer's protocol.

Naive CD4$^+$ Th1, Th2, Th17, and regulatory T cell differentiation in vitro

Naive CD4$^+$ T cells were purified from mice with MicroBeads and differentiated in vitro. For Th1, Th2, Th17, and regulatory T cell (Treg) differentiation, naive CD4$^+$ T cells were incubated with plate-bound mAbs of anti-CD3 and anti-CD28 under Th1 conditions (10 ng/ml IL-12, 1 μg/ml anti–IL-4 mAb), Th2 conditions (10 ng/ml IL-4, 10 μg/ml anti–IFN-γ mAb, 1 μg/ml anti–IL-12 mAb), Th17 conditions (1 μg/ml anti–IL-4 mAb, 10 μg/ml anti–IFN-γ mAb, 20 ng/ml IL-6, 1 ng/ml TGF-β), or Treg conditions (1 ng/ml TGF-β, 50 U/ml IL-2) for 72 h. Differentiated Th cells were washed and restimulated with plate-bound anti-CD3 mAb for 24 h, and cell supernatants were used for measuring cytokine levels by ELISA (R&D Systems).

Generation of CD4-Cre: shp-2$^{flox/flox}$ CD4-specific cell conditional SHP-2 knockout mice

cSHP-2 KO mice were generated by crossing *shp-2*$^{flox/flox}$ mice with CD4-Cre transgenic mice (a gift from Prof. Zichun Hua, Nanjing University) (38).

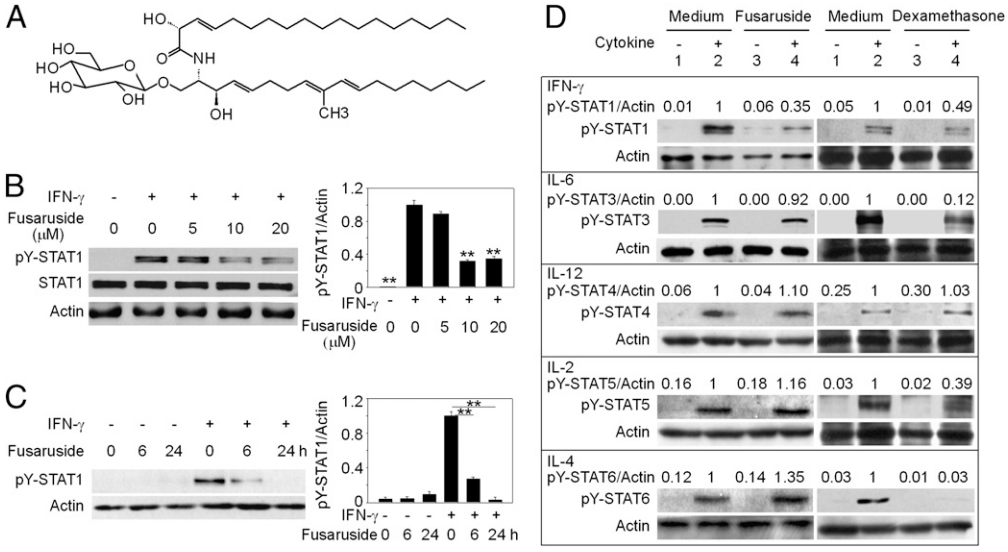

FIGURE 1. Selective inhibition of STAT1 activation among various STAT family members by fusaruside in primary CD4$^+$ T cells. (**A**) The chemical structure of fusaruside. (**B**) T cells were cultured with fusaruside (5, 10, or 20 μM) for 6 h following IFN-γ (25 ng/ml) stimulation for 30 min. The results shown are representative of three experiments. $^{**}p < 0.01$, compared with the IFN-γ control group. (**C**) T cells were cultured with fusaruside (10 μM) for 6 or 24 h. The cells were then treated with murine IFN-γ (25 ng/ml) for 30 min. $^{**}p < 0.01$. (**D**) T cells were cultured without (*lanes 1* and *2*) or with (*lanes 3* and *4*) 10 μM fusaruside/1 μM dexamethasone for 24 h. These cells were then left untreated (*lanes 1* and *3*) or were treated with murine IFN-γ (25 ng/ml), IL-6 (25 ng/ml), IL-12 (5 ng/ml), IL-2 (10 ng/ml), or IL-4 (10 ng/ml) (*lanes 2* and *4*) for 30 min. After these incubations, the proteins were extracted and subjected to Western blot analysis. The results shown are representative of three experiments.

Induction of TNBS-induced colitis in mice and drug administration

Murine colitis was induced by TNBS following a published protocol (39) with some modifications. Briefly, adult male C57BL/6 mice were sensitized with 150 μl 1% TNBS solution on abdominal skin 7 d before challenge. On the day of challenge, mice were lightly anesthetized, and TNBS solution (2.5 mg TNBS in 50% ethanol solution) was administered intrarectally. Sham control mice received 50% ethanol alone. Animals were monitored daily for the loss of body weight and survival. On days 0, 1, and 2, mice were injected i.p. with 2.5, 5, or 10 mg/kg fusaruside or 1 mg/kg dexamethasone in PBS. In another experiment, mice were injected i.p. with 5 mg/kg fusaruside, 5 mg/kg fusaruside plus 5 mg/kg NSC-87877, or 5 mg/kg NSC-87877 in PBS. Control mice received PBS alone.

T cell transfer colitis model

SCID mice were injected i.v. with 5×10^5 $CD4^+$ $CD45RB^{hi}$ T cells. Sham group mice were injected with PBS. Mice were injected i.p. with 2.5 or 5 mg/kg fusaruside in PBS twice a week. Disease progression was monitored by weighing each mouse weekly. When mice lost ~15–20% of their original body weight or at 8 wk after the first injection, they were euthanized and assessed for macroscopic evidence of colitis.

Macroscopic and histologic grading of colitis

Colons and paraffin sections were examined and graded by macroscopic and microscopic analysis following previously reported methods (40, 41). Three days after TNBS administration, mice were sacrificed, and the colon was removed and carefully opened to score colonic damage macroscopically. Nine parameters were taken into account: erythema (0, 1 [<1 cm], 2 [>1 cm]), hemorrhage, edema, stricture formation, ulceration, fecal blood, presence of mucus, diarrhea, and adhesions (0, 1 [mild], 2 [severe]). Each parameter was worth 1 point, with the exception of erythema and adhesions. Grading was performed in a blinded fashion. Histological evaluation of H&E-stained colonic sections was graded in a blinded manner: 0, no signs of inflammation; 1, low leukocyte infiltration; 2, moderate leukocyte infiltration; 3, high leukocyte infiltration, moderate fibrosis, high vascular density, thickening of the colon wall, moderate goblet cell loss, and focal loss of crypts; and 4, transmural infiltrations, massive loss of goblet cell, extensive fibrosis, and diffuse loss of crypts.

ELISA for cytokine production

Cell culture supernatants or serum levels of cytokines were determined using ELISA kits (R&D Systems).

Cytometric Bead Array kits for mouse Th1/Th2/Th17 cytokine production

Cell culture supernatant levels of IL-2, IL-6, TNF-α, IFN-γ, IL-4, IL-17, and IL-10 were determined using cytometric bead array kits (BD Biosciences, San Jose, CA).

Immunoprecipitation, Western blotting, and kinase assay

Proteins from cells (1×10^7) were incubated with 2 μg the appropriate Ab and precipitated with protein A/G-agarose beads (Santa Cruz Biotechnology). The immunoprecipitated proteins were separated by SDS-PAGE, and Western blotting was performed with the indicated Abs. In kinase assays, the coimmunoprecipitates were tested using a JAK2 kinase assay kit (Cell Signaling Technology), according to the manufacturer's protocol.

Real-time RT-PCR analysis

RNA was extracted from cells (5×10^6) or frozen colonic tissues (20 mg) using TRIzol reagent (Invitrogen). One microgram of RNA was

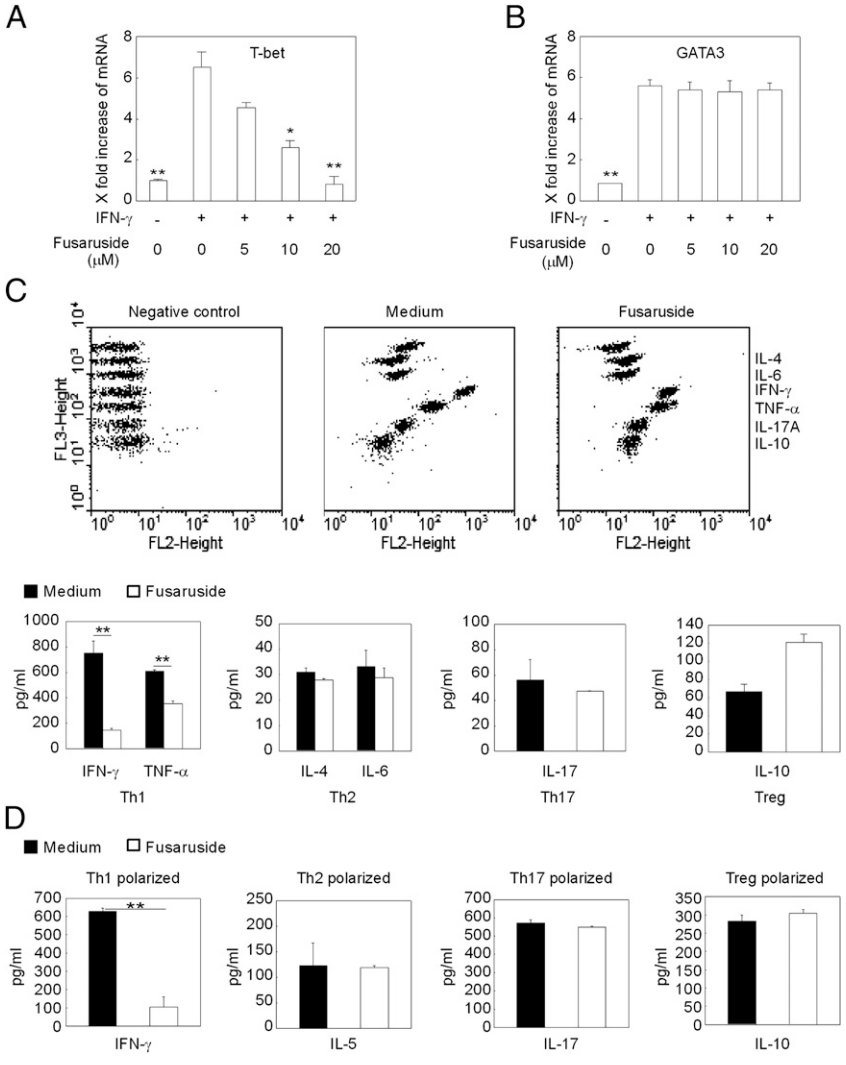

FIGURE 2. Selective inhibition of the expression of the Th1 transcription factor, T-bet, and Th1 cytokine production by fusaruside. (**A**) Real-time PCR analysis of T-bet expression in T cells cultured with or without fusaruside for 6 h and then treated with murine IFN-γ (25 ng/ml) for 6 h. (**B**) Real-time PCR analysis of GATA3 expression in T cells cultured or not with fusaruside for 6 h and then treated with murine IL-4 (25 ng/ml) for 6 h. One-way ANOVA revealed a significant difference ($*p < 0.05$, $**p < 0.01$) compared with the IFN-γ–treated group. (**C**) Culture supernatants from primary T cells stimulated with anti-CD3/anti-CD28 Abs in the presence of 10 μM fusaruside for 48 h were assessed with a mouse Th1/Th2/Th17 cytokine cytometric bead array kit. $**p < 0.01$. (**D**) Polarized Th1, Th2, Th17, and Treg cells were treated or not with fusaruside (10 μM) for 72 h, and culture supernatants were subjected to ELISA. The values represent the mean ± SEM from three independent experiments. $**p < 0.01$.

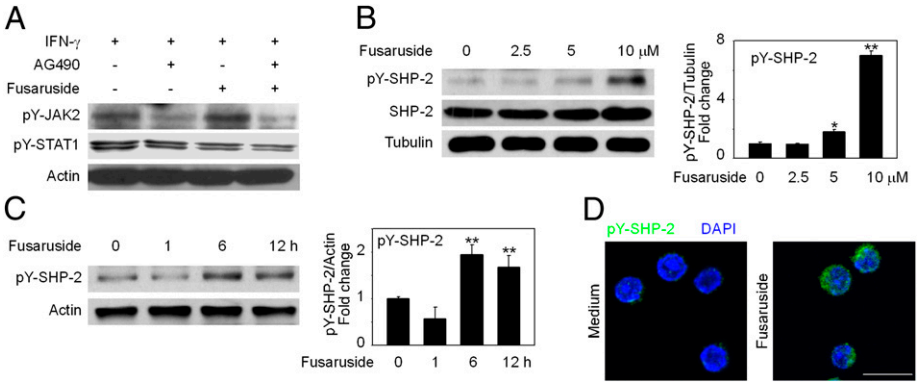

FIGURE 3. Fusaruside induces the tyrosine phosphorylation of SHP-2 without inhibiting the activation of JAK2. (**A**) Splenic T cells were cultured with 10 μM fusaruside and/or 50 μM of the JAK2 inhibitor AG490 for 6 h. The T cells were then treated with IFN-γ (25 ng/ml) for 30 min. After incubation, the cell lysates were subjected to Western blot analysis. The results shown are representative of three experiments. (**B**) Splenic T cells were cultured with 2.5, 5, or 10 μM fusaruside for 6 h. (**C**) Splenic T cells were cultured with 10 μM fusaruside for 1, 6, or 12 h. After treatment, the proteins were subjected to Western blot analysis. (**D**) Splenic T cells were cultured with 10 μM fusaruside for 6 h. After treatment, the cells were analyzed by immunofluorescence cytochemistry (scale bar, 10 μm). The results shown are representative of three experiments. $*p < 0.05$, $**p < 0.01$, compared with the group not treated with fusaruside.

reverse transcribed to cDNA. The primer sequences used in PCR were as follows: GAPDH, 5′-AACGACCCCTTCATTGAC and 3′-CACGACTCATACAGCACCT; T-bet, 5′-CTCAGGTGGCTGGCTTTC and 3′-ATTCGTTCCTGCCGCTTA; and GATA-binding protein 3 (GATA3), 5′-GGGTTCGGATGTAAGTCG and 3′-GTAGGGACTCGGTGTAGA. Reactions were run in triplicate using GAPDH as the internal RNA control on an ABI 7000 Thermocycler (Applied Biosystems, Framingham, MA).

Immunofluorescence histochemistry

Thin cryosections (4 μm) of colonic tissue were fixed in acetone, stained with the primary Ab pY-STAT1 (1:50, raised in rabbit) and anti–CD4-PE (1: 50), and detected with a secondary Ab (Alexa Fluor 488 goat anti-rabbit IgG, 1:500; Invitrogen). The sections were then stained with DAPI and examined with a confocal laser scanning microscope (Olympus, Lake Success, NY).

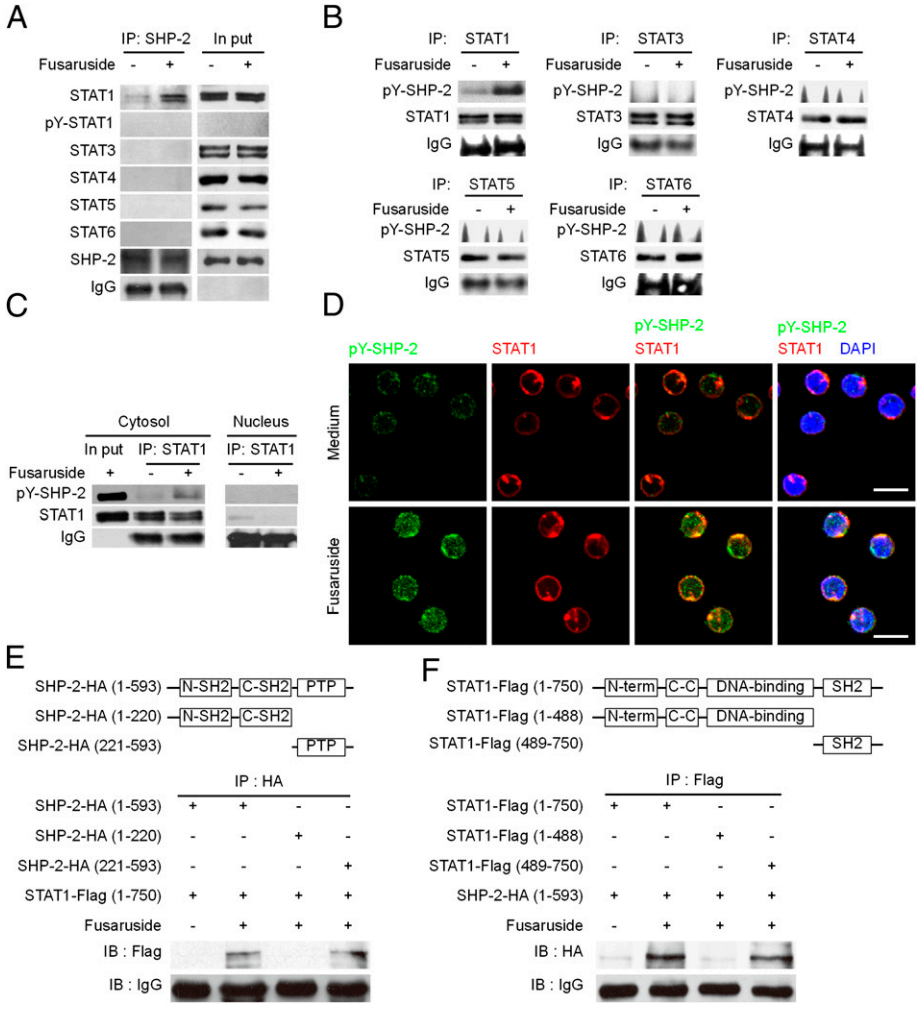

FIGURE 4. Fusaruside induces the interaction between pY-SHP-2 and STAT1 in the cytosol. T cells were treated or not with 10 μM fusaruside for 6 h, and the proteins were isolated and immunoprecipitated with an Ab against SHP-2 (**A**) or Abs against STAT1, STAT3, STAT4, STAT5, or STAT6 (**B**). The immunoprecipitates were then assessed by Western blotting. (**C**) T cells were treated or not with 10 μM fusaruside for 6 h, and the cytosolic and nuclear fractions were then separated for immunoprecipitation and Western blot analysis. (**D**) T cells were treated or not with 10 μM fusaruside for 6 h. After treatment, the cells were analyzed by immunofluorescence cytochemistry (scale bar, 10 μm). (**E** and **F**) The indicated plasmids (3 μg) were transfected into 293T cells. Twenty-four hours later, cells were treated with 10 μM fusaruside for 6 h. After incubation, cells were collected and used for immunoprecipitation experiments. All data shown are representative of three experiments.

Immunofluorescence cytochemistry

Mesenteric lymph node (MLN) T cells adhered to glass coated with BD Cell-Tak Cell and Tissue Adhesive (BD PharMingen) were fixed with 4% paraformaldehyde (40 min, room temperature), stained with the following Abs (STAT1 [C terminus], 1:100 and pY-SHP-2, 1:250), and detected with secondary Abs (Alexa Fluor 488 anti-mouse IgG and Alexa Fluor 594 anti-rabbit IgG, 1:1000; Invitrogen). The coverslips were counterstained with DAPI and imaged with a confocal laser scanning microscope (Olympus).

Flow cytometric analysis of cell surface and intracellular Ags

Freshly isolated MLN cells (1×10^6) were fixed with Fix Buffer I, permeabilized with Perm Buffer III, and stained with anti-pY-STAT1 conjugated with Alexa Fluor 488 and anti-CD4 conjugated with allophycocyanin (all from BD PharMingen). Cells were analyzed with a FACSCalibur flow cytometer (Becton Dickinson, Sunnyvale, CA).

Statistical analysis

Data are expressed as mean ± SEM. Statistical analyses were performed using one-way analysis of variance (ANOVA), followed by Student two-tailed *t* test. Mortality differences between groups were evaluated by the Kaplan–Meier method. Differences with p values ≤ 0.05 are considered significant.

Results

Selective regulation of STAT1 signaling in T cells occurs via the small-molecule compound fusaruside

Fusaruside (Fig. 1A), a novel cerebroside compound isolated from an endophytic fungus in *Quercus variabilis*, was reported to possess antibacterial and xanthine oxidase inhibitory activities (37). We previously screened for the selective immunosuppressive chemicals and found that the effect of fusaruside was quite unique. To assess the regulation of STAT1 signaling by fusaruside, we compared the activation of different STATs in T cells treated with fusaruside. When T cells were stimulated with Th1 cytokine, IFN-γ, we found that phosphorylation, but not expression, of STAT1 was markedly inhibited by fusaruside in a dose-dependent (Fig. 1B) and time-dependent (Fig. 1C) manner. Consistent with its effects on STAT1 activation, fusaruside reduced the expression of the IFN-γ–inducible gene, T-bet, in a dose-dependent fashion (Fig. 2A). Fusaruside did not inhibit the activation of other STATs in T cells, including IL-6–induced STAT3, IL-12–induced STAT4, IL-2–induced STAT5, and IL-4–induced STAT6 (Fig. 1D). However, 1 μM dexamethasone inhibited the activation of STAT1, STAT3, STAT5, and STAT6 (Fig. 1D). In addition, in contrast to the inhibition of STAT1 phosphorylation by fusaruside treatment prior to IFN-γ stimulation, the phosphorylated levels of STAT1 were not influenced when the cells were exposed to fusaruside after IFN-γ stimulation (Supplemental Fig. 1).

Fusaruside inhibits the expression of the IFN-γ–induced Th1 transcription factor, T-bet, and the production of the Th1 cytokine, IFN-γ, in activated or polarized T cells

IFN-γ can induce the expression of T-bet, a transcription factor that directs Th1 lineage commitment (42), and IL-4 can induce the early expression of GATA3, a transcription factor that is crucial to Th2 cytokine production (43). Fusaruside decreased the expression of T-bet induced by IFN-γ in T cells (Fig. 2A) in a dose-dependent manner, without affecting the expression of GATA3 induced by IL-4 (Fig. 2B). The Th1/Th2 and Th17/Treg balance is critical for the maintenance of immune homeostasis (44, 45). To determine whether the selective inhibition of IFN-γ/STAT1 signaling could regulate immune homeostasis, the effects of fusaruside on the expression of Th1, Th2, Th17, and regulatory cytokines in activated and polarized T cells were compared. Production of the Th1 cytokines, IFN-γ and TNF-α, in T cells activated by anti-CD3/anti-CD28 Abs was significantly inhibited

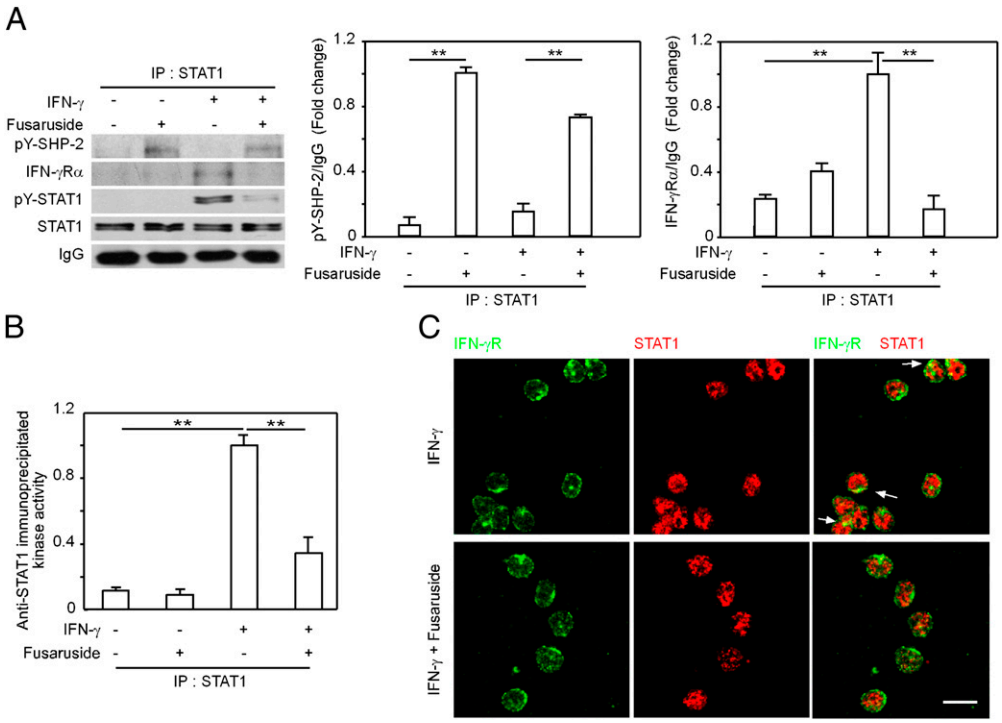

FIGURE 5. The fusaruside-induced interaction between pY-SHP-2 and STAT1 blocks recruitment of STAT1 to IFN-γR during IFN-γ/STAT1 signaling. (**A** and **B**) Lymph node-derived T cells were treated or not with 10 μM fusaruside for 6 h, and the T cells were then treated with 25 ng/ml of IFN-γ for 30 min. After incubation, the total protein was immunoprecipitated with an Ab against STAT1. The immunoprecipitates were assessed by Western blotting (A) and by a JAK2 kinase activity assay (B). (**C**) Lymph node-derived T cells were treated or not with 10 μM fusaruside for 6 h, and the T cells were then treated with 25 ng/ml of IFN-γ for 30 min. After treatment, the cells were analyzed by immunofluorescence cytochemistry (scale bar, 10 μm). The results shown are representative of three experiments. $^{**}p < 0.01$.

by fusaruside; in contrast, production of the Th2 cytokines, IL-4 and IL-6, the regulatory cytokine, IL-10, and the Th17 cytokine, IL-17, was not affected (Fig. 2C). In addition, fusaruside inhibits the production of IFN-γ in Th1-polarized T cells without affecting the production of IL-5 in Th2-polarized T cells, the production of IL-10 in Treg-polarized T cells, or the production of IL-17 in Th17-polarized T cells (Fig. 2D).

Fusaruside initiates the tyrosine phosphorylation of SHP-2

To understand how fusaruside specifically inhibits STAT1 activation, we first examined the effect of fusaruside on the phosphorylation of JAK2. Unlike its inhibition of STAT1 activation, fusaruside did not inhibit IFN-γ–induced JAK2 activation in T cells (Fig. 3A, *lanes 1* and *3*), whereas the JAK2 inhibitor AG490, which was used as a control, decreased the activation of both JAK2 and STAT1 (Fig. 3A, *lanes 1* and *2*). In addition, fusaruside did not affect the mRNA expression of other negative regulators of STAT1, such as SOCS1 (46), protein inhibitor of activated STAT1 (47), or β-arrestin 1 (48) (Supplemental Fig. 2). Next, we examined the effect of fusaruside on SHP-2, which was reported to dephosphorylate pSTAT1 in nuclei (33). We found that SHP-2 was activated by phosphorylation by fusaruside in lymph node-derived T cells in a dose- and time-dependent manner, whereas the total expression of SHP-2 was not affected (Fig. 3B, 3C). As shown in Fig. 3C, there was no obvious increase in the phosphorylation of SHP-2 in T cells treated with fusaruside for 1 h, whereas increased pY-SHP-2 was clearly detected in T cells treated with fusaruside for 6 h. Therefore, we used 6 h of treatment in the following experiments. This finding suggests that the phosphorylation of SHP-2 by fusaruside is a small molecule-mediated event that might be different from current kinase reactions. Immunofluorescence analysis was performed to confirm that fusaruside induced the tyrosine phosphorylation of SHP-2. There were clear increases in the intensity of the fluorescent signal (green), corresponding to phosphorylated SHP-2, in lymph node-derived T cells treated with fusaruside. Interestingly, phosphorylated SHP-2 was located in the cytosol (Fig. 3D). The fusaruside-induced phosphorylation was specific to SHP-2, because the phosphorylation of SHP-1 was not detectable in T cells treated with fusaruside (data not shown).

pY-SHP-2 selectively binds to nonphosphorylated STAT1 in the cytosol

To investigate the function of fusaruside-induced pY-SHP-2, we examined the interactions between SHP-2 and different STATs. It was reported that SHP-2 is associated with and dephosphorylates STAT1 and STAT5 (33, 34). In this study, STAT1, but not pY-STAT1, STAT3, STAT4, STAT5, or STAT6, was detected in anti–SHP-2 immunoprecipitates from fusaruside-treated cells (Fig. 4A). In addition, only pY-SHP-2 was found in anti-STAT1 immunoprecipitates from fusaruside-treated cells; it was not found in anti-STAT3, anti-STAT4, anti-STAT5, or anti-STAT6 immunoprecipitates (Fig. 4B). Furthermore, fusaruside-induced pY-SHP-2 was only detected in anti-STAT1–immunoprecipitated cytosolic proteins (Fig. 4C), and the immunofluorescence showed a greater overlap of STAT1 (green) and pY-SHP-2 (red) (colocalization, yellow), indicating an increased interaction of pY-SHP-2 with STAT1 in the cytosol of T cells treated with fusaruside (Fig. 4D). Moreover, fusaruside failed to induce the interaction between SHP-2 and STAT1 in 293T cells transfected with either the pCMV-SHP-2-HA-N (1–220) or pRc/CMV-STAT1α Flag-N region (1–488), suggesting that the SHP-2 PTP domain and the STAT1-C region are critical for the fusaruside-mediated association between pY-SHP-2 and STAT1 (Fig. 4E, 4F).

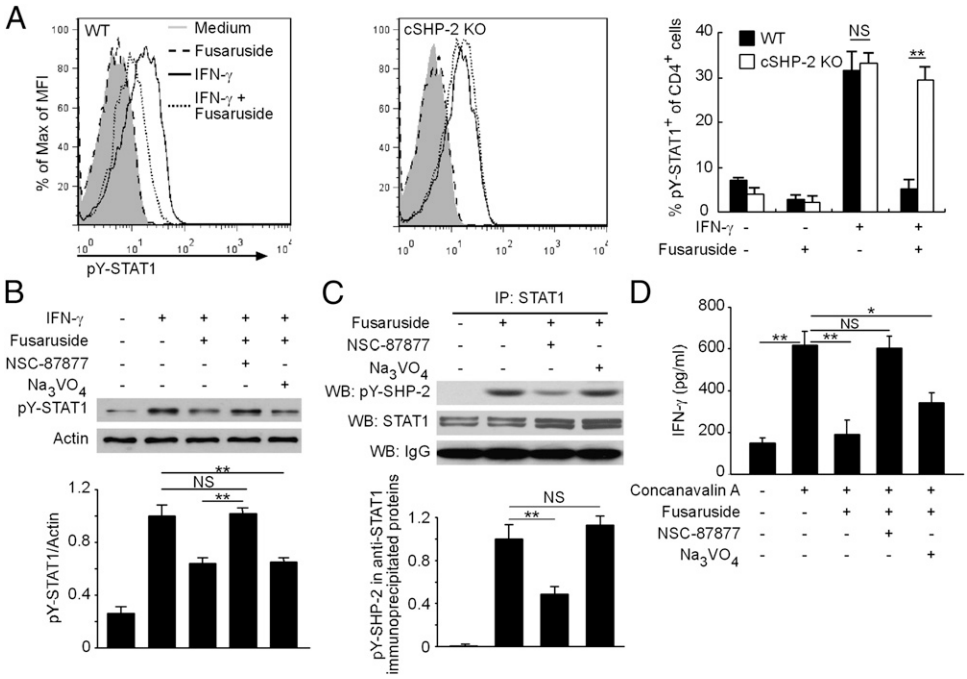

FIGURE 6. Dependency of the fusaruside-induced inhibition of STAT1 activation on the interaction between SHP-2 and STAT1 in T cells. (**A**) Flow cytometric analysis of the effect of fusaruside on the expression of intracellular pY-STAT1 in lymph node cells stimulated with IFN-γ from wild-type or cSHP-2 KO mice. (**B**) Lymph node-derived T cells were treated with 15 μM NSC-87877 or 100 μM Na_3VO_4 for 24 h, incubated with 10 μM fusaruside for 6 h, and then treated or not with 25 ng/ml IFN-γ for 30 min. The cell extracts were then subjected to Western blot analysis. (**C**) Lymph node-derived T cells were treated with 15 μM NSC-87877 or 100 μM Na_3VO_4 for 24 h and incubated with 10 μM fusaruside for 6 h. The cell extracts were then subjected to Western blot analysis. The results shown in (A–C) are representative of three experiments. (**D**) Lymph node-derived T cells stimulated with 5 μg/ml Con A were cotreated with 10 μM fusaruside in the presence of 15 μM NSC-87877 or 100 μM Na_3VO_4 for 24 h. The culture supernatants were then assessed by ELISA. $*p < 0.05$, $**p < 0.01$.

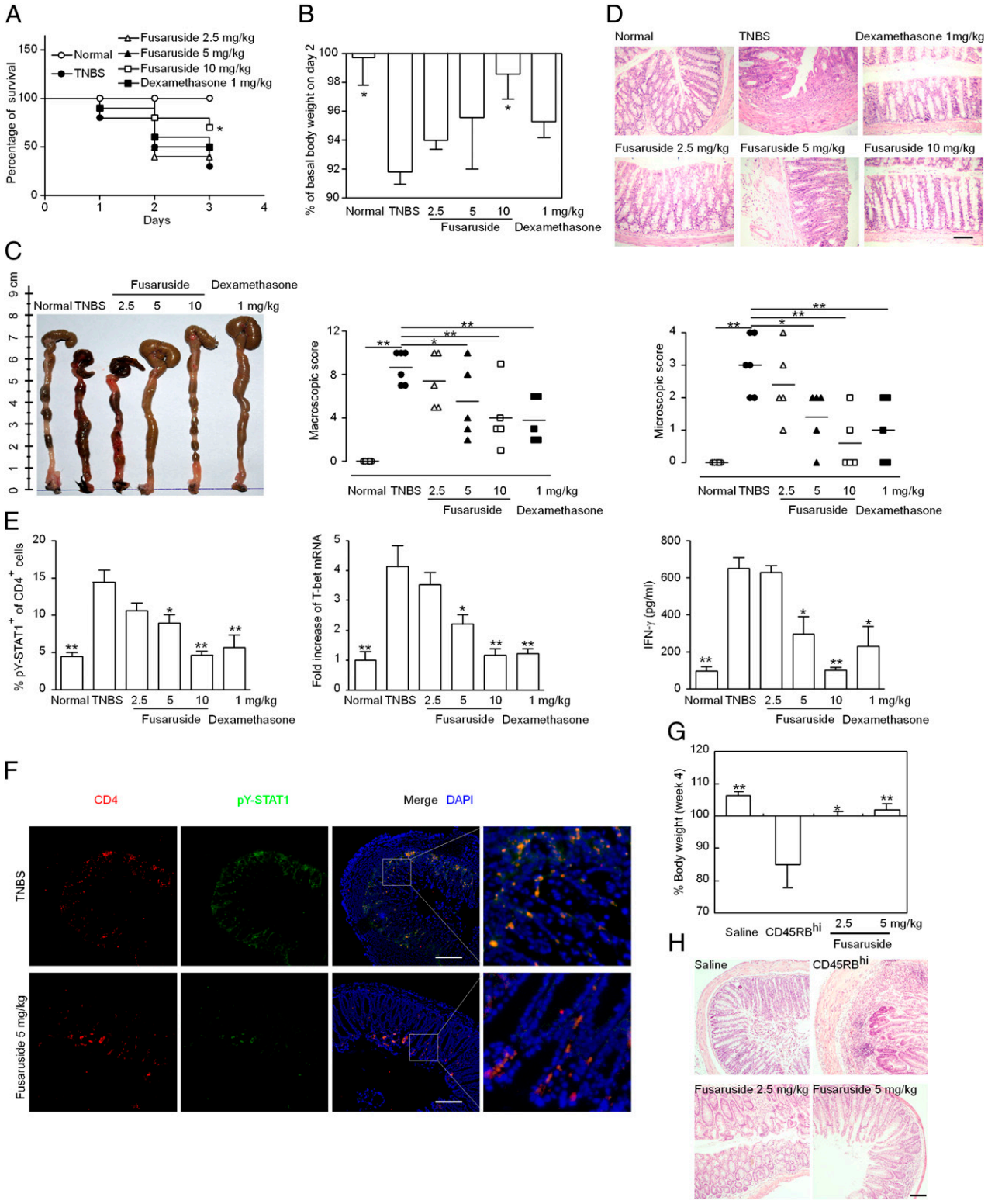

FIGURE 7. Improvement of experimental colitis via the inhibition of IFN-γ/STAT1/T-bet signaling by fusaruside. (**A**) The effect of fusaruside on the survival rate of mice given a TNBS enema. Mortality differences between groups were evaluated by the Kaplan–Meier method. Each group contained 10–12 mice. Disease severity was monitored by body weight changes on day 2 (**B**) and macroscopic damage scores (**C**). (**D**) Histopathologic analyses were performed on H&E-stained sections of colons (scale bar, 100 μm). (**E**) MLN cells were analyzed for CD4 and intracellular pY-STAT1 expression by flow cytometry. The plots were gated on $CD4^+$ T cells, and the percentage of pY-STAT1–expressing $CD4^+$ T cells was determined (bar graphs). The mRNA expression of T-bet in the colon tissue was measured by real-time PCR. The concentration of IFN-γ in the serum was determined by ELISA. The data represent the mean ± SEM of five or six animals. $*p < 0.05$, $**p < 0.01$, compared with TNBS-treated mice, one-way ANOVA. (**F**) Confocal imaging of pY-STAT1 (green), CD4 (red), and DAPI (blue) in colonic tissue (scale bar, 100 μm). The arrows indicate the nuclear location of pY-STAT1. (**G**) Body weight changes at week 4 in a $CD4^+$ $CD45RB^{hi}$ T cell transfer-induced colitis model. The data represent the mean ± SEM of 4–5 animals. $*p < 0.05$, $**p < 0.01$, compared with SCID mice reconstituted with $CD4^+$ $CD45RB^{hi}$ T cells, one-way ANOVA. (**H**) Histopathologic analyses were performed on H&E-stained sections of colonic tissues (scale bar, 100 μm).

pY–SHP-2 sequestrates STAT1 to block its recruitment to IFN-γR and prevent IFN-γ/STAT1/T-bet signaling

We next examined the consequence of this unique association between pY-SHP-2 and STAT1 in STAT1-mediated signaling. In the proteins immunoprecipitated by the anti-STAT1 Ab from IFN-γ–treated T cells, IFN-γRα was detected, suggesting that STAT1 was recruited to the receptor. However, the receptor protein became almost undetectable after treatment with fusaruside in parallel with SHP-2 activation (Fig. 5A). In addition, the kinase activity was greatly reduced in the anti-STAT1–immunoprecipitated proteins (Fig. 5B). Immunofluorescence analysis was performed to confirm that fusaruside blocks STAT1 recruitment to IFN-γR. There was a clear reduction in the intensity of the fluorescent signal (yellow) in T cells that were treated with fusaruside, which corresponded to the interaction between STAT1 and the IFN-γR (Fig. 5C). Thus, the data suggest that the pY-SHP-2 induced by fusaruside sequestrates STAT1 from activation and, thereby, selectively regulates STAT1 signaling.

To determine whether the inhibition of STAT1 activation depends on the interaction between pY-SHP-2 and STAT1, we used T cells from cSHP-2 KO mice and the SHP-2 competitive inhibitor, NSC-87877, to block the binding of STAT1 to pY-SHP-2. The deletion of SHP-2 in $CD4^+$ T cells from cSHP-2 KO mice was confirmed by PCR, immunoblotting analysis, immunocytochemical staining, and flow cytometric analysis (Supplemental Fig. 3). In the $CD4^+$ T cells from cSHP-2 KO mice, the inhibitory effect of fusaruside on STAT1 activation was greatly reduced (Fig. 6A). Furthermore, the above-mentioned effects of fusaruside in lymph node-derived T cells were blocked by the SHP-2 competitive inhibitor, NSC-87877, but not by the tyrosine phosphatase inhibitor, Na_3VO_4. The effects that were blocked included the inhibition of STAT1 phosphorylation (Fig. 6B), the interaction between pY-SHP-2 and STAT1 (Fig. 6C), and the inhibition of IFN-γ production (Fig. 6D).

Fusaruside selectively inhibits Th1-biased experimental colitis

The specific effect of fusaruside on STAT1 signaling was further examined for its potential to ameliorate Th1-mediated colitis in mice. In TNBS-induced colitis, weight loss was commonly observed, and ~40% of the animals survived through day 3. Daily treatments with 10 mg/kg of fusaruside significantly reversed the weight loss and improved the survival rate to 70%, which was greater than the 40% survival rate observed in our positive control group that was given 1 mg/kg dexamethasone (Fig. 7A, 7B). A significant increase in the macroscopic damage scores and colon wall thickness was observed in the mice with colitis. In contrast, a significant attenuation of these responses was found in the colons of mice treated with either 5 or 10 mg/kg of fusaruside or with 1 mg/kg dexamethasone (Fig. 7C). Histological analysis showed that the main characteristics of colitis in the colonic specimens were the distortion of crypts, loss of goblet cells, infiltration of mononuclear cells, and severe mucosal damage. Such changes in the colon tissues were markedly improved by administration of 5 and 10 mg/kg of fusaruside and 1 mg/kg of dexamethasone; the improvement included a marked reduction in inflammatory cell infiltration and mucosal ulcerations (Fig. 7D).

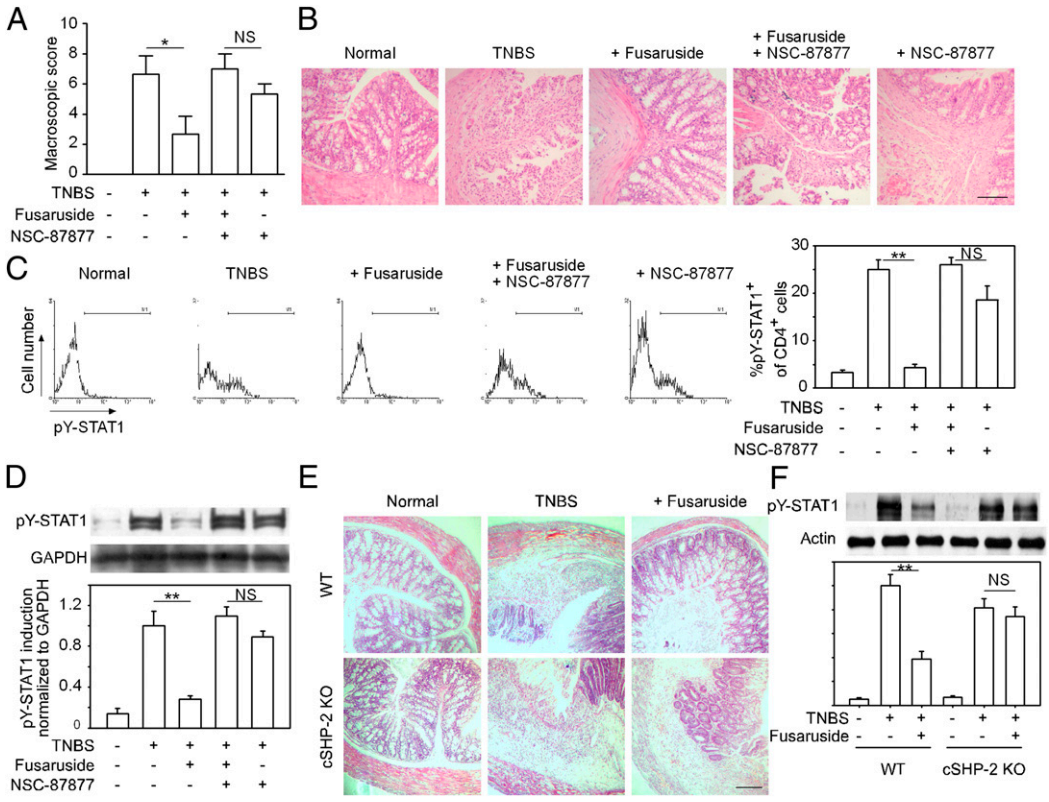

FIGURE 8. Dependency of the improvement of colitis by fusaruside on the interaction between SHP-2 and STAT1. (**A**) Macroscopic damage score. (**B**) Microphotographs of H&E-stained paraffin-embedded sections of distal colonic tissues (scale bar, 100 μm). (**C**) Flow cytometric analysis of STAT1 (pY701) expression in $CD4^+$ T cells from MLNs. The graphs were gated on $CD4^+$ T cells, and the percentage of pY-STAT1–expressing cells in $CD4^+$ T cells was determined (bar graph). (**D**) Western blot analysis of pY-STAT1 and GAPDH expression in MLN cells. Data are mean ± SEM of experimental animals ($n = 6$). (**E** and **F**) Colitis was induced by TNBS in wild-type (WT) and cSHP-2 KO mice. (E) Microphotograph of H&E-stained paraffin-embedded sections of distal colonic tissues (scale bar, 100 μm). (F) Western blot analysis of pY-STAT1 and actin expression in MLN cells. Data are mean ± SEM of experimental animals ($n = 6$). A significant difference was revealed following one-way ANOVA analysis (*$p < 0.05$, **$p < 0.01$).

MLN cells were isolated, and the percentage of phosphorylated STAT1$^+$ cells in the CD4$^+$ T cell population was examined using intracellular staining. Fusaruside-treated mice with colitis showed a dose-dependent reduction in the number of pY-STAT1$^+$ CD4$^+$ T cells, and normal levels of pY-STAT1 were achieved at the 10 mg/kg dose. Likewise, fusaruside inhibited T-bet mRNA expression in colonic tissue in a dose-dependent manner (Fig. 7E). Confocal imaging revealed that pY-STAT1 (green) was strongly expressed and was localized in the nuclei of colonic CD4$^+$ cells in mice with TNBS-induced colitis. Fusaruside (5 mg/kg) markedly reduced the nuclear expression of pY-STAT1 in CD4$^+$ cells (Fig. 7F). In addition, fusaruside ameliorated the colitis induced by transfer of CD4$^+$ CD45RB^{hi} T cells (Fig. 7G, 7H).

pY-SHP-2–STAT1 interaction contributes to the improvement of experimental colitis observed in fusaruside-treated mice

The SHP-2 inhibitor, NSC-87877 (5 mg/kg), was injected i.p. into mice to block the binding of pY-SHP-2 to STAT1 in vivo. The resolution of colitis by fusaruside observed by macroscopic and histological analysis was mostly abolished by NSC-87877 (Fig. 8A, 8B). Furthermore, the decrease in the expression of pY-STAT1 in MLN T cells treated with fusaruside was completely reversed by NSC-87877 (Fig. 8C, 8D). Histological analyses showed that fusaruside failed to improve TNBS-induced colitis in cSHP-2 KO mice (Fig. 8E) and that fusaruside could not inhibit STAT1 activation in MLN T cells from cSHP-2 KO mice with TNBS-induced colitis (Fig. 8F). Consistently, fusaruside failed to prevent the loss of body weight and inhibit serum IFN-γ production in cSHP-2 KO mice (Supplemental Fig. 4). Thus, the improvement of TNBS-induced colitis by fusaruside depends on the pY-SHP-2–STAT1 interaction.

All above results could be summarized as a novel mode of STAT1 regulation. In brief, the cerebroside fusaruside triggers the phosphorylation of SHP-2. The phosphorylated SHP-2 sequestrates STAT1 from recruitment to IFN-γR and thereby inhibits the STAT1/T-bet signaling, which contributes to the amelioration of inflammatory colitis (Fig. 9).

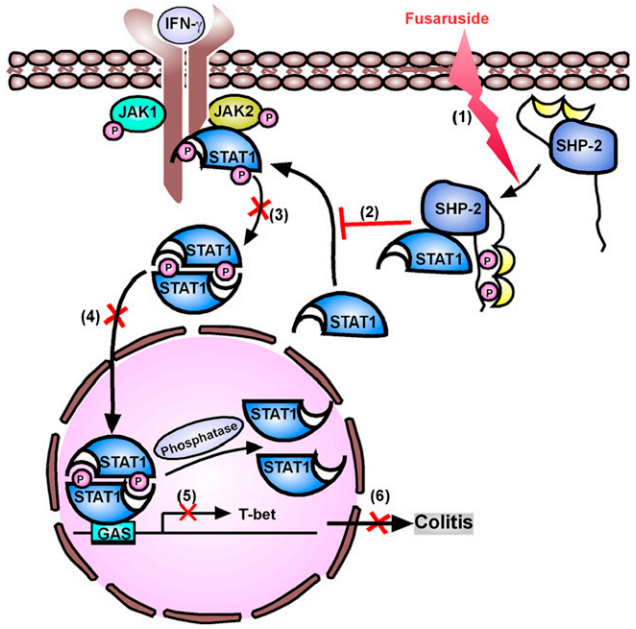

FIGURE 9. A novel mode of STAT1 regulation by the fusaruside-driven, SHP-2–mediated sequestration of STAT1. (**1**) The phosphorylation of SHP-2 and the interaction between pY-SHP-2 and nonphosphorylated STAT1 in the cytosol were triggered by fusaruside. (**2**) Recruitment of STAT1 to IFN-γR during IFN-γ signaling was blocked by pY-SHP-2. STAT1 homodimerization (**3**) and nuclear translocation (**4**) were also inhibited. (**5**) The expression of T-bet downstream of STAT1 signaling was inhibited by fusaruside. (**6**) TNBS-induced colitis was ameliorated by fusaruside.

Discussion

In this study, we report a novel protein–protein interaction that regulates STAT1 signaling; the interaction is induced by the small molecule compound, fusaruside, which causes the selective tethering of nonphosphorylated STAT1 in the cytosol by pY-SHP-2. This constitutive interaction between pY-SHP-2 and STAT1 has not been reported and is different from a previous report that found that SHP-2 dephosphorylates pY-STAT1 in the nucleus of A431 cells (33). Our conclusions are based on the following observations. First, only the nonphosphorylated form of STAT1 was detected in SHP-2 coimmunoprecipitates from fusaruside-treated T cell extracts (Fig. 4A), and pY-SHP-2 was only found in STAT1 coimmunoprecipitates from fusaruside-treated T cell cytosolic extracts (Fig. 4C). Second, pY-SHP-2 was detected by immunofluorescence microscopy in the cytosol (Fig. 3D), and it colocalized with cytosolic STAT1, but not nuclear STAT1, in fusaruside-treated T cells (Fig. 4D). Third, the SHP-2 competitive inhibitor, NSC-87877, blocked the pY-SHP-2–STAT1 interaction, thereby reversing the inhibition of STAT1 activation by fusaruside; in contrast, the tyrosine phosphatase inhibitor, Na_3VO_4, could not reverse this inhibition (Fig. 6B, 6C). These data suggest that STAT1 inhibition depends on the fusaruside-induced interaction between pY-SHP-2 and STAT1 but not on the phosphatase activity of pY-SHP-2. Accordingly, there was no inhibition of STAT1 activation by fusaruside in T cells from cSHP-2 KO mice (Fig. 6A). Fourth, in contrast to the inhibition of STAT1 phosphorylation by fusaruside treatment prior to IFN-γ stimulation, the phosphorylated levels of STAT1 were not affected when the cells were exposed to fusaruside after IFN-γ stimulation (Supplemental Fig. 1), which suggests that fusaruside requires time to induce the interaction between pY-SHP-2 and STAT1 that inhibits STAT1 activation. These results show conclusively that triggering the constitutive binding of pY-SHP-2 to STAT1 by a small-molecule compound is a novel method of STAT1 regulation; additionally, the interaction of SHP-2 with nonphosphorylated STAT1 is a new biological activity for SHP-2 and extends beyond its role in dephosphorylation. Stewart et al. (36) also reported that SHP-2 has functions in addition to its phosphatase activity. However, the nonphosphatase function of SHP-2 is largely unknown.

Targeting the interaction between pY–SHP-2 and STAT1 is specific and is different from targeting the enzymatic activity of SHP-2 or JAK2. SHP-2 is known to dephosphorylate STAT1 and STAT5 (33, 34). In contrast, neither pY-STAT1 nor other STAT members, including STAT3, STAT4, STAT5, and STAT6, were detected in anti-SHP-2 immunoprecipitates from fusaruside-treated cells (Fig. 4A). In addition, increased levels of pY–SHP-2 were only found in anti-STAT1 immunoprecipitates, but not in anti-STAT3, STAT4, STAT5, or STAT6 immunoprecipitates, from fusaruside-treated cells (Fig. 4B). JAK2 can activate multiple STAT members, such as STAT1, STAT3, STAT5a, and STAT6 (4). Thus, the inhibition of JAK2 causes the suppression of multiple STAT signals. We found that fusaruside did not reduce the phosphorylation of JAK2 induced by IFN-γ in T cells (Fig. 3A), which confirmed the selectivity of fusaruside in targeting STAT1 signaling without influencing JAK2. Interestingly, with regard to IFN-γ–induced signaling, neither IFN-γR (Fig. 5A) nor kinase (Fig. 5B) was detected in proteins immunoprecipitated from fusaruside-treated cells using the anti-STAT1 Ab. This suggests that once fusaruside triggers the pY-SHP-2–STAT1 interaction,

STAT1 is blocked from recruitment to the kinase for phosphorylation. These results confirm that STAT1 is sequestered by pY–SHP-2, which keeps STAT1 in its latent form, shielding it from stimulation by IFN-γ and, thereby, preventing STAT1 signaling.

This novel regulation of STAT1 signaling presents a unique scenario for the treatment of Th1 cell-mediated inflammatory diseases. The specificity of fusaruside targeting of STAT1 signaling was validated by showing the selective inhibition of STAT1 phosphorylation but not total STAT1 expression; the selective inhibition of STAT1 activation but not STAT3, STAT4, STAT5, or STAT6 activation; and the selective inhibition of Th1 cytokine production and T-bet expression but not Th2 cytokine production or GATA3 expression. To the best of our knowledge, the ability of fusaruside to selectively inhibit STAT1 activation and the Th1 immune response distinguishes it from other current drugs, such as dexamethasone, cyclosporin A, and FK506. Dexamethasone, a well-known immunosuppressive drug that was used as the control for comparing selectivity, inhibited almost all of the STAT family members, including STAT1, STAT3, STAT5, and STAT6, in splenic T cells (Fig. 1D). Cyclosporin A and FK506 inhibited both the Th1 and Th2 immune responses (49–51). Fusaruside showed a significant resolution of TNBS-induced colitis in mice by inhibiting IFN-γ/STAT1/T-bet signaling (Fig. 7), which depended on the pY-SHP-2–STAT1 interaction (Fig. 8). These findings confirmed downregulation of the IFN-γ/STAT1/T-bet–signaling pathway by fusaruside and the critical role of this pathway in Th1-type colitis. In this study, the inhibition of IFN-γ/STAT1 signaling by fusaruside in T cells and in colonic tissues was linked to the resolution of TNBS-induced colitis and was evidenced by reduced IFN-γ/STAT1 signaling, Th1 immune responses, and Th1-mediated inflammation in mice.

In summary, the unique molecule fusaruside selectively inhibits STAT1 signaling in T cells without suppressing other STAT family members. Using this compound, we reveal a novel process in T cells in which phosphorylated SHP-2 sequestrates STAT1 to prevent signaling through the molecule (Fig. 9). This new function of SHP-2 is in addition to its classical role as a phosphatase and contributes to the selective regulation of Th1-type immune responses and inflammation. Hence, the specific targeting of a critical STAT member as a novel therapeutic approach in Crohn's disease and other Th1-type inflammatory diseases has been discovered, and this specificity has advantages over current therapies because of its potential to reduce side effects.

Acknowledgments

We thank Dr. Prof. Zichun Hua (Nanjing University) for providing CD4-Cre mice.

Disclosures

The authors have no financial conflicts of interest.

References

1. José León, A., J. A. Garrote, and E. Arranz. 2006. [Cytokines in the pathogenesis of inflammatory bowel diseases]. *Med. Clin. (Barc.)* 127: 145–152.
2. Bandyopadhyay, S. K., C. A. de la Motte, S. P. Kessler, V. C. Hascall, D. R. Hill, and S. A. Strong. 2008. Hyaluronan-mediated leukocyte adhesion and dextran sulfate sodium-induced colitis are attenuated in the absence of signal transducer and activator of transcription 1. *Am. J. Pathol.* 173: 1361–1368.
3. Neurath, M. F., B. Weigmann, S. Finotto, J. Glickman, E. Nieuwenhuis, H. Iijima, A. Mizoguchi, E. Mizoguchi, J. Mudter, P. R. Galle, et al. 2002. The transcription factor T-bet regulates mucosal T cell activation in experimental colitis and Crohn's disease. *J. Exp. Med.* 195: 1129–1143.
4. Schindler, C. W. 2002. Series introduction. JAK-STAT signaling in human disease. *J. Clin. Invest.* 109: 1133–1137.
5. O'Shea, J. J., M. Pesu, D. C. Borie, and P. S. Changelian. 2004. A new modality for immunosuppression: targeting the JAK/STAT pathway. *Nat. Rev. Drug Discov.* 3: 555–564.
6. Leng, C., M. Gries, J. Ziegler, A. Lokshin, P. Mascagni, S. Lentzsch, and M. Y. Mapara. 2006. Reduction of graft-versus-host disease by histone deacetylase inhibitor suberonylanilide hydroxamic acid is associated with modulation of inflammatory cytokine milieu and involves inhibition of STAT1. *Exp. Hematol.* 34: 776–787.
7. Frank, D. A., S. Mahajan, and J. Ritz. 1999. Fludarabine-induced immunosuppression is associated with inhibition of STAT1 signaling. *Nat. Med.* 5: 444–447.
8. Plaza, R., S. Vidal, J. L. Rodriguez-Sanchez, and C. Juarez. 2004. Implication of STAT1 and STAT3 transcription factors in the response to superantigens. *Cytokine* 25: 1–10.
9. Kristof, A. S., J. Marks-Konczalik, E. Billings, and J. Moss. 2003. Stimulation of signal transducer and activator of transcription-1 (STAT1)-dependent gene transcription by lipopolysaccharide and interferon-gamma is regulated by mammalian target of rapamycin. *J. Biol. Chem.* 278: 33637–33644.
10. Hu, X., W.-P. Li, C. Meng, and L. B. Ivashkiv. 2003. Inhibition of IFN-gamma signaling by glucocorticoids. *J. Immunol.* 170: 4833–4839.
11. Ben Ya'acov, A., G. Lalazar, D. M. Livovsky, D. Kanovich, E. Axelrod, S. Preston, G. Schwarzmann, and Y. Ilan. 2009. Decreased STAT-1 phosphorylation by a thio analogue of beta-D-glucosylceramide is associated with altered NKT lymphocyte polarization. *Mol. Immunol.* 47: 526–533.
12. McCubrey, J. A., W. S. May, V. Duronio, and A. Mufson. 2000. Serine/threonine phosphorylation in cytokine signal transduction. *Leukemia* 14: 9–21.
13. Kusaba, H., P. Ghosh, R. Derin, M. Buchholz, C. Sasaki, K. Madara, and D. L. Longo. 2005. Interleukin-12-induced interferon-gamma production by human peripheral blood T cells is regulated by mammalian target of rapamycin (mTOR). *J. Biol. Chem.* 280: 1037–1043.
14. Cristillo, A. D., and B. E. Bierer. 2002. Identification of novel targets of immunosuppressive agents by cDNA-based microarray analysis. *J. Biol. Chem.* 277: 4465–4476.
15. Han, S. B., S. H. Park, Y. J. Jeon, Y. K. Kim, H. M. Kim, and K. H. Yang. 2001. Prodigiosin blocks T cell activation by inhibiting interleukin-2Ralpha expression and delays progression of autoimmune diabetes and collagen-induced arthritis. *J. Pharmacol. Exp. Ther.* 299: 415–425.
16. Henttinen, T., D. E. Levy, O. Silvennoinen, and M. Hurme. 1995. Activation of the signal transducer and transcription (STAT) signaling pathway in a primary T cell response. Critical role for IL-6. *J. Immunol.* 155: 4582–4587.
17. Bianchi, M., C. Meng, and L. B. Ivashkiv. 2000. Inhibition of IL-2-induced Jak-STAT signaling by glucocorticoids. *Proc. Natl. Acad. Sci. USA* 97: 9573–9578.
18. Franchimont, D., J. Galon, M. Gadina, R. Visconti, Y. J. Zhou, M. Aringer, D. M. Frucht, G. P. Chrousos, and J. J. O'Shea. 2000. Inhibition of Th1 immune response by glucocorticoids: dexamethasone selectively inhibits IL-12-induced Stat4 phosphorylation in T lymphocytes. *J. Immunol.* 164: 1768–1774.
19. Zigmond, E., S. Preston, O. Pappo, G. Lalazar, M. Margalit, Z. Shalev, L. Zolotarov, D. Friedman, R. Alper, and Y. Ilan. 2007. Beta-glucosylceramide: a novel method for enhancement of natural killer T lymphocyte plasticity in murine models of immune-mediated disorders. *Gut* 56: 82–89.
20. Park, C., S. Li, E. Cha, and C. Schindler. 2000. Immune response in Stat2 knockout mice. *Immunity* 13: 795–804.
21. El Kasmi, K. C., J. Holst, M. Coffre, L. Mielke, A. de Pauw, N. Lhocine, A. M. Smith, R. Rutschman, D. Kaushal, Y. Shen, et al. 2006. General nature of the STAT3-activated anti-inflammatory response. *J. Immunol.* 177: 7880–7888.
22. Takeda, K., B. E. Clausen, T. Kaisho, T. Tsujimura, N. Terada, I. Förster, and S. Akira. 1999. Enhanced Th1 activity and development of chronic enterocolitis in mice devoid of Stat3 in macrophages and neutrophils. *Immunity* 10: 39–49.
23. Gao, B. 2005. Cytokines, STATs and liver disease. *Cell. Mol. Immunol.* 2: 92–100.
24. Pernis, A. B., and P. B. Rothman. 2002. JAK-STAT signaling in asthma. *J. Clin. Invest.* 109: 1279–1283.
25. Elrod, J. W., F. S. Laroux, J. Houghton, A. Carpenter, T. Ando, M. H. Jennings, M. Grisham, N. Walker, and J. S. Alexander. 2005. DSS-induced colitis is exacerbated in STAT-6 knockout mice. *Inflamm. Bowel Dis.* 11: 883–889.
26. van Meeteren, M. E., M. A. C. Meijssen, and F. J. Zijlstra. 2000. The effect of dexamethasone treatment on murine colitis. *Scand. J. Gastroenterol.* 35: 517–521.
27. You, M., D. H. Yu, and G. S. Feng. 1999. Shp-2 tyrosine phosphatase functions as a negative regulator of the interferon-stimulated Jak/STAT pathway. *Mol. Cell. Biol.* 19: 2416–2424.
28. An, H., W. Zhao, J. Hou, Y. Zhang, Y. Xie, Y. Zheng, H. Xu, C. Qian, J. Zhou, Y. Yu, et al. 2006. SHP-2 phosphatase negatively regulates the TRIF adaptor protein-dependent type I interferon and proinflammatory cytokine production. *Immunity* 25: 919–928.
29. Kim, H. Y., E. J. Park, E. H. Joe, and I. Jou. 2003. Curcumin suppresses Janus kinase-STAT inflammatory signaling through activation of Src homology 2 domain-containing tyrosine phosphatase 2 in brain microglia. *J. Immunol.* 171: 6072–6079.
30. Chan, R. J., and G. S. Feng. 2007. PTPN11 is the first identified proto-oncogene that encodes a tyrosine phosphatase. *Blood* 109: 862–867.
31. Tartaglia, M., S. Martinelli, L. Stella, G. Bocchinfuso, E. Flex, V. Cordeddu, G. Zampino, I. Burgt, A. Palleschi, T. C. Petrucci, et al. 2006. Diversity and functional consequences of germline and somatic PTPN11 mutations in human disease. *Am. J. Hum. Genet.* 78: 279–290.
32. Bard-Chapeau, E. A., S. Li, J. Ding, S. S. Zhang, H. H. Zhu, F. Princen, D. D. Fang, T. Han, B. Bailly-Maitre, V. Poli, et al. 2011. Ptpn11/Shp2 acts as a tumor suppressor in hepatocellular carcinogenesis. *Cancer Cell* 19: 629–639.
33. Wu, T. R., Y. K. Hong, X. D. Wang, M. Y. Ling, A. M. Dragoi, A. S. Chung, A. G. Campbell, Z. Y. Han, G. S. Feng, and Y. E. Chin. 2002. SHP-2 is a dual-specificity phosphatase involved in Stat1 dephosphorylation at both tyrosine and serine residues in nuclei. *J. Biol. Chem.* 277: 47572–47580.

34. Yu, C. L., Y. J. Jin, and S. J. Burakoff. 2000. Cytosolic tyrosine dephosphorylation of STAT5. Potential role of SHP-2 in STAT5 regulation. *J. Biol. Chem.* 275: 599–604.
35. Yu, W. M., T. S. Hawley, R. G. Hawley, and C. K. Qu. 2003. Catalytic-dependent and -independent roles of SHP-2 tyrosine phosphatase in interleukin-3 signaling. *Oncogene* 22: 5995–6004.
36. Stewart, R. A., T. Sanda, H. R. Widlund, S. Zhu, K. D. Swanson, A. D. Hurley, M. Bentires-Alj, D. E. Fisher, M. I. Kontaridis, A. T. Look, and B. G. Neel. 2010. Phosphatase-dependent and -independent functions of Shp2 in neural crest cells underlie LEOPARD syndrome pathogenesis. *Dev. Cell* 18: 750–762.
37. Shu, R. G., F. W. Wang, Y. M. Yang, Y. X. Liu, and R. X. Tan. 2004. Antibacterial and xanthine oxidase inhibitory cerebrosides from *Fusarium* sp. IFB-121, an endophytic fungus in *Quercus variabilis*. *Lipids* 39: 667–673.
38. Orban, P. C., D. Chui, and J. D. Marth. 1992. Tissue- and site-specific DNA recombination in transgenic mice. *Proc. Natl. Acad. Sci. USA* 89: 6861–6865.
39. Wirtz, S., C. Neufert, B. Weigmann, and M. F. Neurath. 2007. Chemically induced mouse models of intestinal inflammation. *Nat. Protoc.* 2: 541–546.
40. Cenac, N., A. M. Coelho, C. Nguyen, S. Compton, P. Andrade-Gordon, W. K. MacNaughton, J. L. Wallace, M. D. Hollenberg, N. W. Bunnett, R. Garcia-Villar, et al. 2002. Induction of intestinal inflammation in mouse by activation of proteinase-activated receptor-2. *Am. J. Pathol.* 161: 1903–1915.
41. Fiorucci, S., J. L. Wallace, A. Mencarelli, E. Distrutti, G. Rizzo, S. Farneti, A. Morelli, J. L. Tseng, B. Suramanyam, W. J. Guilford, and J. F. Parkinson. 2004. A beta-oxidation-resistant lipoxin A4 analog treats hapten-induced colitis by attenuating inflammation and immune dysfunction. *Proc. Natl. Acad. Sci. USA* 101: 15736–15741.
42. Szabo, S. J., S. T. Kim, G. L. Costa, X. Zhang, C. G. Fathman, and L. H. Glimcher. 2000. A novel transcription factor, T-bet, directs Th1 lineage commitment. *Cell* 100: 655–669.
43. Murphy, K. M., and S. L. Reiner. 2002. The lineage decisions of helper T cells. *Nat. Rev. Immunol.* 2: 933–944.
44. Kidd, P. 2003. Th1/Th2 balance: the hypothesis, its limitations, and implications for health and disease. *Altern. Med. Rev.* 8: 223–246.
45. Afzali, B., G. Lombardi, R. I. Lechler, and G. M. Lord. 2007. The role of T helper 17 (Th17) and regulatory T cells (Treg) in human organ transplantation and autoimmune disease. *Clin. Exp. Immunol.* 148: 32–46.
46. Alexander, W. S., R. Starr, J. E. Fenner, C. L. Scott, E. Handman, N. S. Sprigg, J. E. Corbin, A. L. Cornish, R. Darwiche, C. M. Owczarek, et al. 1999. SOCS1 is a critical inhibitor of interferon gamma signaling and prevents the potentially fatal neonatal actions of this cytokine. *Cell* 98: 597–608.
47. Liu, B., J. Liao, X. Rao, S. A. Kushner, C. D. Chung, D. D. Chang, and K. Shuai. 1998. Inhibition of Stat1-mediated gene activation by PIAS1. *Proc. Natl. Acad. Sci. USA* 95: 10626–10631.
48. Mo, W., L. Zhang, G. Yang, J. Zhai, Z. Hu, Y. Chen, X. Chen, L. Hui, R. Huang, and G. Hu. 2008. Nuclear beta-arrestin1 functions as a scaffold for the dephosphorylation of STAT1 and moderates the antiviral activity of IFN-gamma. *Mol. Cell* 31: 695–707.
49. Fei, M., X. Wu, and Q. Xu. 2005. Astilbin inhibits contact hypersensitivity through negative cytokine regulation distinct from cyclosporin A. *J. Allergy Clin. Immunol.* 116: 1350–1356.
50. Bundick, R. V., R. I. Craggs, and E. Holness. 1995. The effect of cyclosporin A, FK506, and rapamycin on the murine chronic graft-versus-host response—an in vivo model of Th2-like activity. *Clin. Exp. Immunol.* 99: 467–472.
51. Sugiyama, M., M. Funauchi, T. Yamagata, Y. Nozaki, B. S. Yoo, S. Ikoma, K. Kinoshita, and A. Kanamaru. 2004. Predominant inhibition of Th1 cytokines in New Zealand black/white F1 mice treated with FK506. *Scand. J. Rheumatol.* 33: 108–114.